



*Research article*

## Photovoltaic power generation enhancement performance with a LDR-based dual-axis solar tracking system

**Zongjin Li<sup>1</sup>, Chi Liu<sup>1</sup>, Guoyang Song<sup>1</sup>, Defa Han<sup>2</sup>, Yingge Li<sup>1,2</sup> and Dongxing Du<sup>1,\*</sup>**

<sup>1</sup> Geo-Energy Research Institute, College of Electromechanical Engineering, Qingdao University of Science and Technology, Gaomi 261550, China

<sup>2</sup> College of Automation and Electronic Engineering, Qingdao University of Science and Technology, Qingdao 266100, China

\* Correspondence: Email: du-dongxing@qust.edu.cn.

**Abstract:** In this work, the enhancement of the solar cell output in a light-dependent resistor (LDR)-based dual-axis solar tracking system (DASTS) in a fixed solar panel system was quantified under different seasons and weather conditions in the city of Qingdao, China. Measurement results show that DASTS could significantly improve power generation efficiency, providing 9.9%–12.8% and 30.6%–32.8% extra daily power output over a fixed-angle system in winter and spring, respectively. It was also found that the power output of the solar panel is higher during the noon period of winter than in spring. Special attention was therefore placed on the effect of panel temperature on the solar panel photovoltaic (PV) conversion efficiency. A clear inverse relationship was observed between the two factors, with the PV conversion efficiency decreasing from 14.7% to 9.8% with an increased panel temperature from 20 to 55 °C. It is concluded that, to achieve maximum solar cell panel power output, the panel temperature effect needs to be taken into consideration.

**Keywords:** solar cell; dual-axis sun tracking system; enhancement performance; panel temperature effect; power output

---

### 1. Introduction

The heavy dependence of human society on fossil fuels has led to a large amount of greenhouse gas emissions, which not only exacerbate global climate change but also pose a threat to public health [1,2].

Technologies aiming to mitigate greenhouse gas emissions and recycling utilizations are therefore becoming a hot research spot [3–7]. Among various emerging clean energy technologies, solar photovoltaic (PV) power generation stands as an important branch to simultaneously fulfill carbon neutrality and green economy transformation [8–10].

In order to maximize the reception of solar radiation, solar tracking systems (STS) with single-axis or dual-axis structures that synchronize to the movement of the sun are becoming a popular research topic [11–15]. Among the representative single-axis solar tracking system (SASTS) studies, Wang et al. [16] improved a tilted bifacial PV system and reported an annual power gain ratio up to 30%. Khandekar et al. [17] developed an intelligent system to drive the SASTS and reported a higher power conversion efficiency of 30.3% against 22.4% in a fixed panel system. On the other hand, the dual-axis solar tracking system (DASTS) has found wider applications than the SASTS as it can track the maximum sun irradiation direction in a more precise manner [18–22]. In comparison with the normal fixed panel setup, Fathabadi [23] reported 19.1%–30.2% higher solar energy capture amount in different seasons via employing an offline sensor-less DASTS. Sidek et al. [24] reported a 26.9% higher power generation by employing astronomical and GPS data to achieve dual-axis sun tracking. Jamroen et al. [25] obtained 20% higher energy generation with a UV sensor-based DASTS. Ponce-Jara et al. [26] demonstrated that the DASTS based on IoT technology could generate extra 19.6% electricity energy. To maximize sun irradiance collection under unfavorable weather conditions, Andriamahefa et al. [27] combined a radiometric cube with four photodiode sensors to control the dual-axis sun tracker movement, based on which they achieved extra 40.5% energy in cloudy days. Jaafar et al. [28] reported that the DASTS would improve the energy output by up to 45%. In an additional comparison to SASTS, Nguyen and Ho [29] recorded an outstanding performance of the DASTS, 20.7% and 32.4% over the single-axis and fixed system, respectively. Even with a novel structure design, Zhu [30] found that the SASTS could only achieve 96.4% performance of the dual-axis system. Riyadi et al. [31] reported a collected solar radiation of 7.523 kWh/m<sup>2</sup>/d from DASTS, obviously higher than that from fixed (5.639 kWh/m<sup>2</sup>/d) and one-axis solar systems (6.858 kWh/m<sup>2</sup>/d).

Although it has been well demonstrated that the DASTS could more efficiently collect solar power, the complexity of the movement system and maintenance costs make the dual-axis system lack commercial competitiveness in comparison to the single-axis and/or fixed panel systems that have simpler mechanical parts and/or control algorithms [32]. Following the microcontroller's instruction to improve altitude and azimuth tracking efficiency, more energy consumption with additional external power input is usually required to activate the DASTS motor than the fixed panel system [33–36]. To alleviate concerns about DASTS' cost and complexity, several novel designs and implementations have been reported in recent years. For instance, Jamroen et al. [37] presented a digital logic-designed automatic DASTS based on a closed-loop control algorithm and four LDR sensors. They found that the proposed tracking system could increase energy harvest efficiency by 44.89% against the fixed panel systems at a revenue time of 754–1130 days, depending on the different electricity prices of 0.3–0.2 \$/kWh. Karabiber and Guñes [38] designed an asymmetric solar tracker (AST) system that is free from heavy metal parts and activated by a single motor. They declared that it had the same cost level as fixed panel systems but could provide 25%–38% extra daily energy output. Song et al. [39] designed an LDR sensor-based DASTS driven by panel self-generated electricity without any external power supply. Their tests showed that it could generate 28.5%–42.9% more power output than the fixed system at a cost-benefit period of 10 years at an electricity price of 0.15 \$/kWh.

It can be deduced from the above literature studies that, in order to maximize the photovoltaic

conversion efficiency, the DASTS has prevailed in recent years. Its design, implementation, and performance, however, vary among researchers. Additionally, the mechanical and control systems and the specifications of the employed solar panels differ significantly among works, and comprehensive performance evaluations of DASTS in different seasons are not widely available.

To help achieve higher solar power collection efficiency and widen the knowledge of solar energy conversion behaviors, in this work, the enhancement performance of a solar panel in an LDR-based DASTS is quantified in both winter and spring. Based on the measurement results, the effect of the panel temperature on solar energy conversion efficiency is also investigated. It is expected that this study could comprehensively clarify the performance of DASTS and reveal key factors for PV conversion efficiency, thus contributing to an increasingly sustainable society.

## 2. Experimental analysis

### 2.1. DASTS

Descriptions of the design and fabrication of the LDR-based DASTS are displayed in Figure 1 for the front and back views, respectively. Figure 1(a) shows the key component of the LDR sensor and polycrystalline solar panel at a size of  $1533 \times 657 \text{ mm}^2$ . Figure 1(b) clearly reveals the mechanical and control parts of the DASTS.

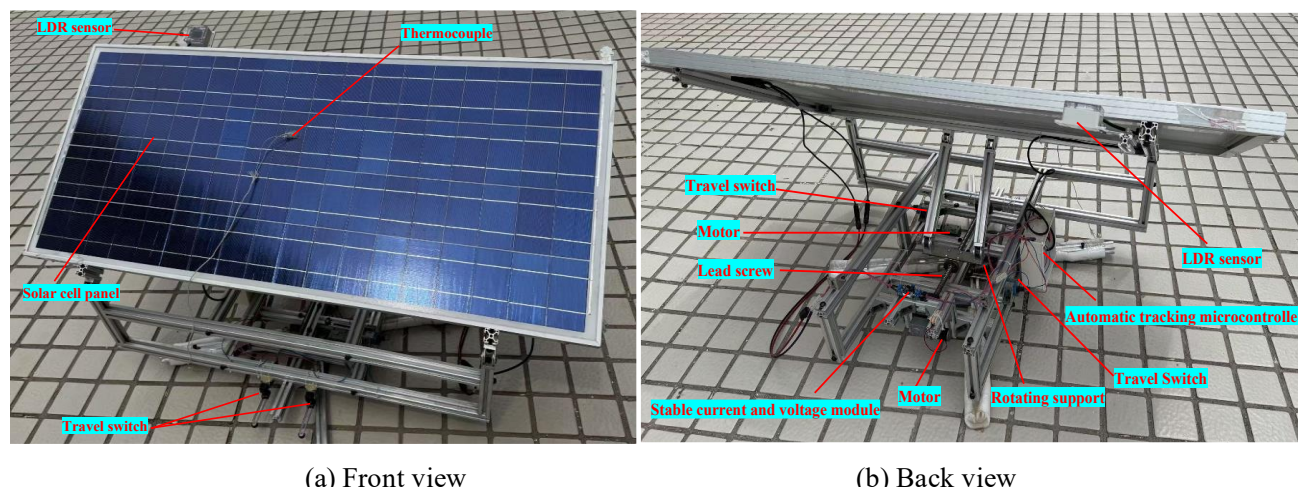


**Figure 1.** Illustration of the LDR sensor-based DASTS.

Figure 2 details the key mechanical and control parts of the DASTS. For an accurate positioning in response to radiation direction, the LDR unit consists of four light-dependent resistor sensors that comprehensively evaluate the received light intensity. The microcontroller is able to activate the two separate motors to adjust the orientation of the solar panels via two movements: inclination and rotation. The solar auto-tracker can also manually adjust the solar panel orientation to suit different operational needs, such as keeping the panel at a certain inclination and direction. It is worth noting that there is no external power supply to operate the microcontroller and the two motors. In all weather conditions, dual-axis position adjustments are fulfilled through the electricity generated by the solar panel itself, which ensures the net power gain of the DASTS.

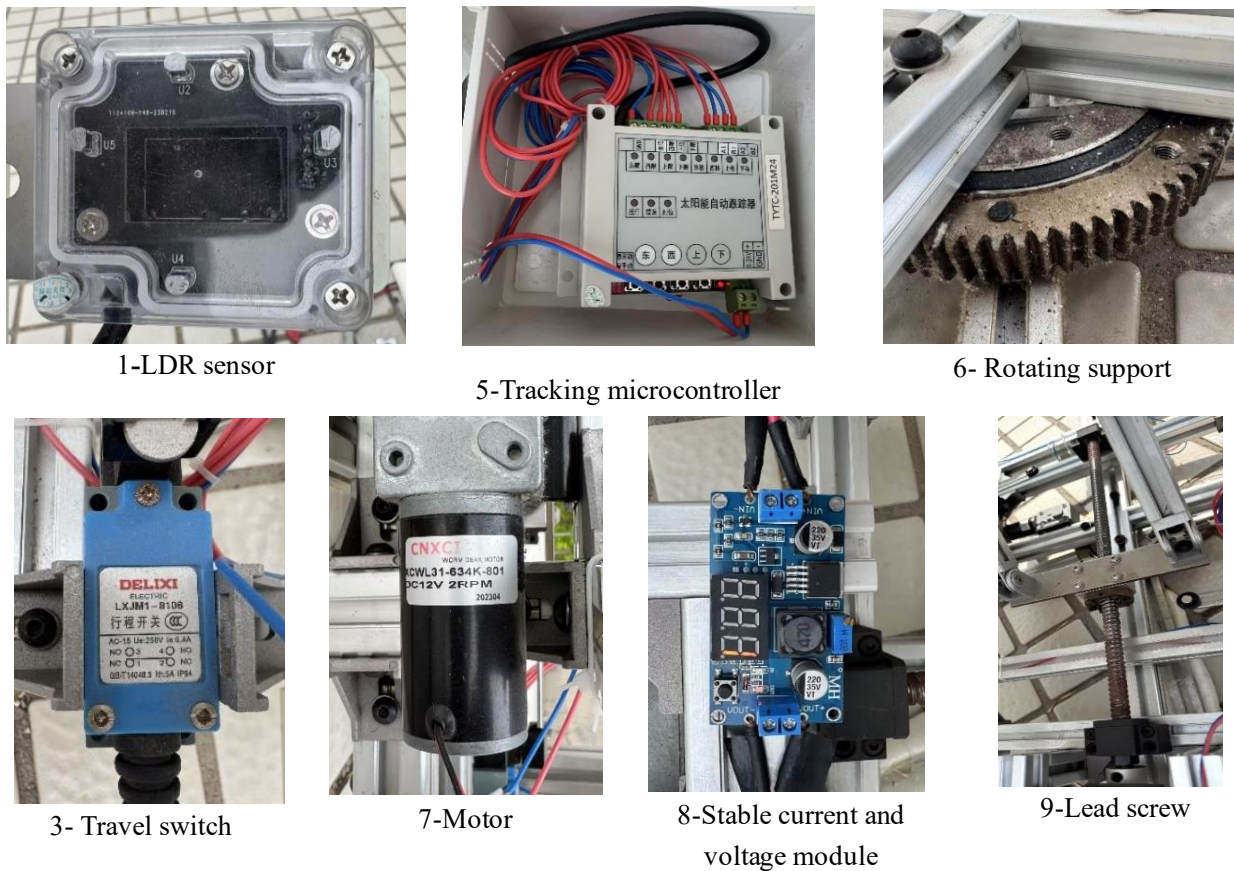


**Figure 2.** Key parts in the DASTS fabrication.

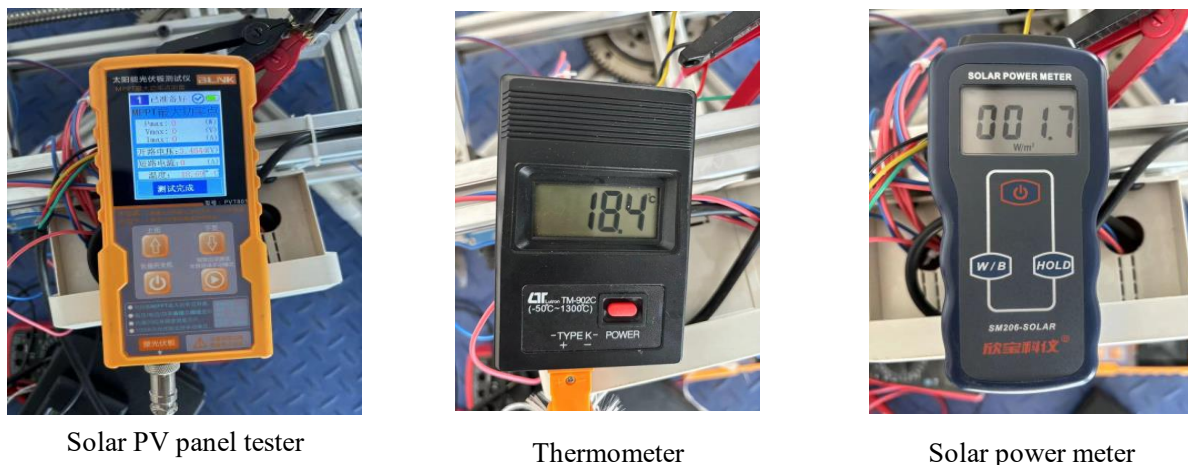


**Figure 3.** Measurement devices for evaluating the DASTS performance.

Figure 3 describes the measurement devices for the key parameters of solar panel power generation, panel temperature, and solar irradiation intensity. Specifically, the solar PV panel tester or maximum power point tracker (MPPT) can track the maximum power point and accurately measure the power output of the solar panel, while the solar power meter can provide instantaneous sun radiation intensity.

## 2.2. Measurement procedures

Measurements were conducted to evaluate the solar PV power output of the DASTS compared to a fixed solar panel system during winter and spring seasons between January and May, 2024, in the City of Qingdao, East China. The DASTS ensures that the solar panel is always perpendicular to the direction of solar radiation, while the stationary system fixes the solar panel facing south at a tilt angle. Based on the season and location of the city, the azimuth angle of the stationary system was set to 2° south by west, and the tilt angle was set to 34°. To compare the power output enhancement performance of the DASTS with the stationary system, after measurement on DASTS, the auto-tracking controller was turned off, and the solar panel was reset to the stationary position to obtain the power output of the fixed solar panel. The two sets of measurements were carried out under the same weather conditions to ensure reliable comparative studies. In this study, the power output of the DASTS and the fixed system were measured in the winter and spring; additional parameters, such as panel temperature and light intensity perpendicular to the direction of the solar panel, were measured in the spring. Based on the actual time of sunrise and sunset from January to May in the testing site, the measurement period was set to 8:00–17:00 with data acquisition every 15 min.

## 3. Results and discussions

### 3.1. Test dates and weather conditions

Table 1 lists the specific weather conditions, including air temperature, wind level, and wind direction, for each test date: January 28 and 30 in the winter, and March 31, April 9, 16, and 24, and May 1, 2, and 3 in the spring. The weather is described as sunny (favorable), cloudy to sunny (common), or cloudy (unfavorable), to ensure a comprehensive evaluation and analysis of the energy collection enhancement performance of the DASTS over the fixed panel system. By including different weather conditions in different seasons, it is expected that the test results will fully explore the advantages of DASTS in the enhancement of solar power utilization.

**Table 1.** Test dates and weather conditions.

Dates	Weather conditions	Temperature	Wind power (scale)	Wind direction
2024.1.28	Sunny	-2–4 °C	2	Northwest
2024.1.30	Cloudy	4–7 °C	3	Southeast
2024.3.31	Cloudy to Sunny	8–14 °C	2	Southeast
2024.4.9	Sunny	10–17 °C	2	Southeast
2024.4.16	Cloudy to Sunny	9–23 °C	1	Northwest
2024.4.24	Cloudy to Sunny	13–21 °C	2	Northwest
2024.5.1	Sunny	12–25 °C	2	Southwest
2024.5.2	Cloudy	11–24 °C	2	South
2024.5.3	Foggy to Sunny	13–20 °C	2	South

### 3.2. PV outputs at different seasons

#### 3.2.1. PV output in the winter

Solar panel power output from both the DASTS and the fixed panel system was measured on January 28 and 30 during winter; the results for both days are depicted in Figure 4(a),(b), respectively. DASTS' highest power output during the sunny day of January 28 was nearly 120 W, much higher than the maximum 100 W during the cloudy day of January 30. The DASTS could also capture solar energy more efficiently, especially in the morning and the afternoon period, than the fixed solar panel system. Even under cloudy weather, as is the case in Figure 4(b), the DASTS provided an increase in power output compared to the stationary system, demonstrating that DASTS is able to function under unfavorable cloudy weather conditions.

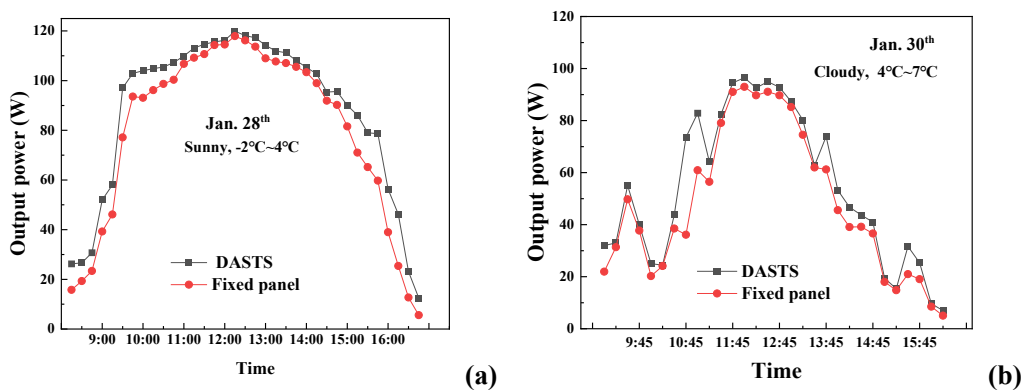


**Figure 4.** Comparison of the PV output power between DASTS and the fixed panel system during the winter days of (a) January 28 and (b) January 30.

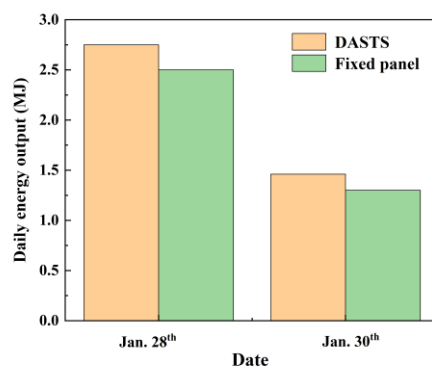


**Figure 5.** Comparison of the daily PV power output between DASTS and the fixed panel system during the winter days of January 28 and January 30.

Based on the electricity generation power output results shown in Figures 4 and 5, it is evident that both systems had higher power output on January 28 than on January 30 due to the higher sunlight

intensity. It is also observed from the figure that, on the sunny day of January 28, the DASTS generated power at 2.75 MJ versus 2.50 MJ of the stationary system; on the cloudy day of January 30, the power generated by DASTS was 1.46 MJ, higher than the 1.30 MJ provided by the stationary system. It can be estimated that the power output of the DASTS was 9.9% higher than that of the stationary system on a sunny day and 12.8% higher on a cloudy day, showing a more obvious enhancement performance of the DASTS on cloudy days during winter.

### 3.2.2. PV output in the spring

Figure 6 shows the power output profiles of the DASTS and the stationary solar panel system during several days of spring: March 31, April 9, April 16, and April 24. The power output of the stationary system, as depicted in red lines, shows a clear dependence on the degree of deviation to the maximum sun irradiation direction, with a clearly lower power generation in the morning (8:30–10:30) and afternoon (14:30–16:30) periods, when the sun irradiation direction is far from the fixed direction in the stationary panel system. On the other hand, the power output behavior of the DASTS, in black lines, shows obvious improvements in the two periods of the day with a much flatter power output profile, clearly demonstrating the outperformance of DASTS over the fixed panel system.

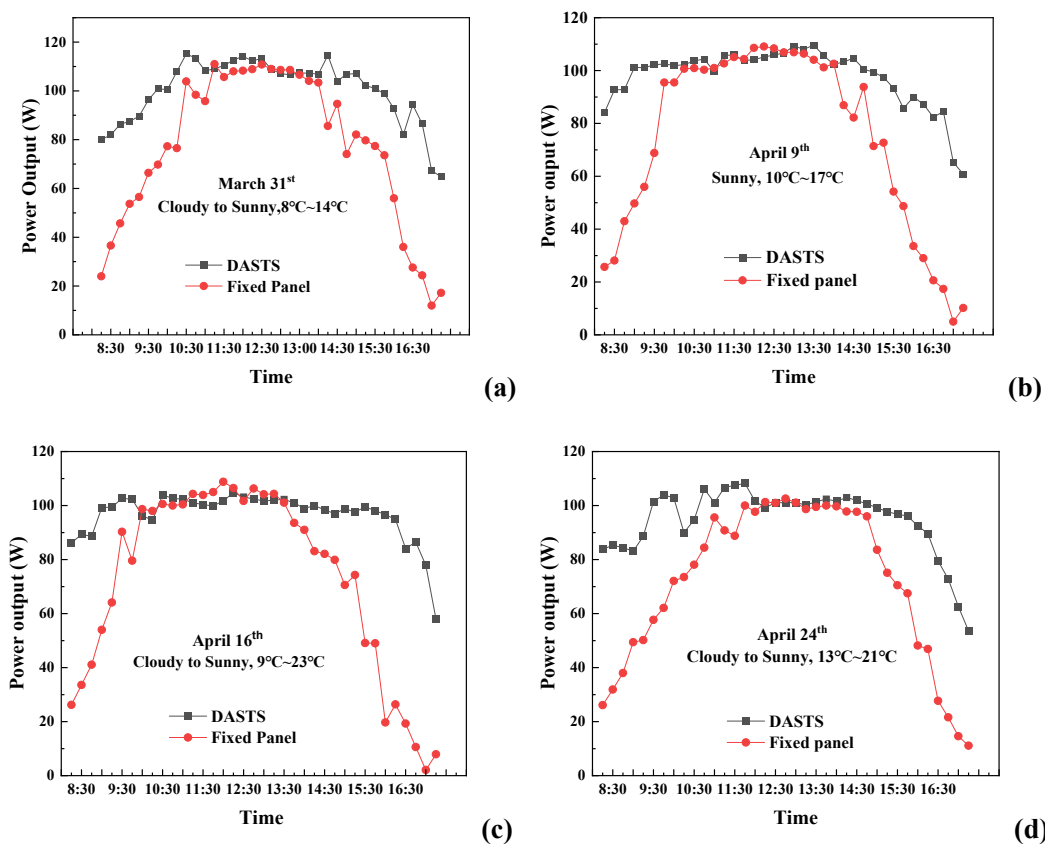


**Figure 6.** Comparison of the PV output power between the DASTS and the fixed panel system during spring days of (a) March 31, (b) April 9, (c) April 16, and (d) April 24.

Figure 7 compares the daily power output from both solar panel systems during the four days in the spring. It is clearly observed that the DASTS significantly improved the power output compared to the stationary system, with a generated power of 3.33, 3.25, 3.22, and 3.15 MJ compared with 2.55, 2.48, 2.42, and 3.15 MJ on March 31, April 9, April 16, and April 24, respectively. The enhancement ratio of the DASTS was 30.6%–31.8% higher than that of the fixed panel system. In comparison to Figure 5, which shows the results during winter, both the energy output and the enhanced performance of DASTS were much more significant during spring. It is concluded, therefore, that the DASTS could provide more electricity power than the stationary panel system regardless of season and weather conditions.

It is worth noting that the measurement results on daily power generation output amount, as well as the enhancement ratio of the DASTS over the stationary system obtained here, agree with literature data in the spring season of 2023 [39], thus validating the results reported in this study.

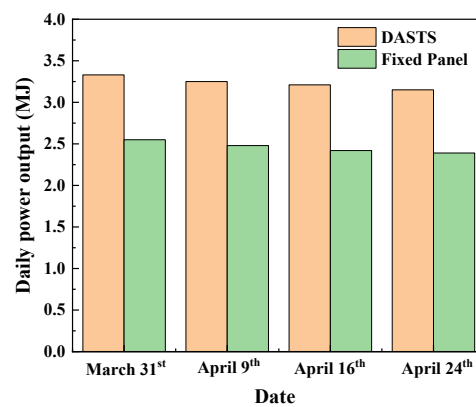


**Figure 7.** Comparison of the daily PV power output between the DASTS and the fixed panel system during the spring days of March 31, April 9, April 16, and April 24.

### 3.3. Effect of panel temperature on the PV output performance

The PV output power profiles in winter, as shown in Figure 4, and in spring, as shown in Figure 6, show that although the overall power output was lower in winter, the output powers of DASTS at the midday hours between 11:00 am and 1:00 pm in winter were comparable to those in the spring. It is expected that, in addition to the sun radiation intensity, other factors influence the solar panel power output behavior. After analyzing the weather conditions in these days, as listed in Table 1, we see that the temperatures during January 28 and 30 were clearly lower, by 15–19 °C, than those during the spring days. As such, it was deduced that panel temperature could also play a role in the PV electricity power output performance. Accordingly, in this section, the panel temperature effect on PV output power and PV conversion efficiency is studied.

#### 3.3.1. PV power output

To reveal the effect of panel temperature on the solar panel power output, both panel temperatures and instantaneous generation power in the four days of spring are plotted in Figure 8(a)–(d).

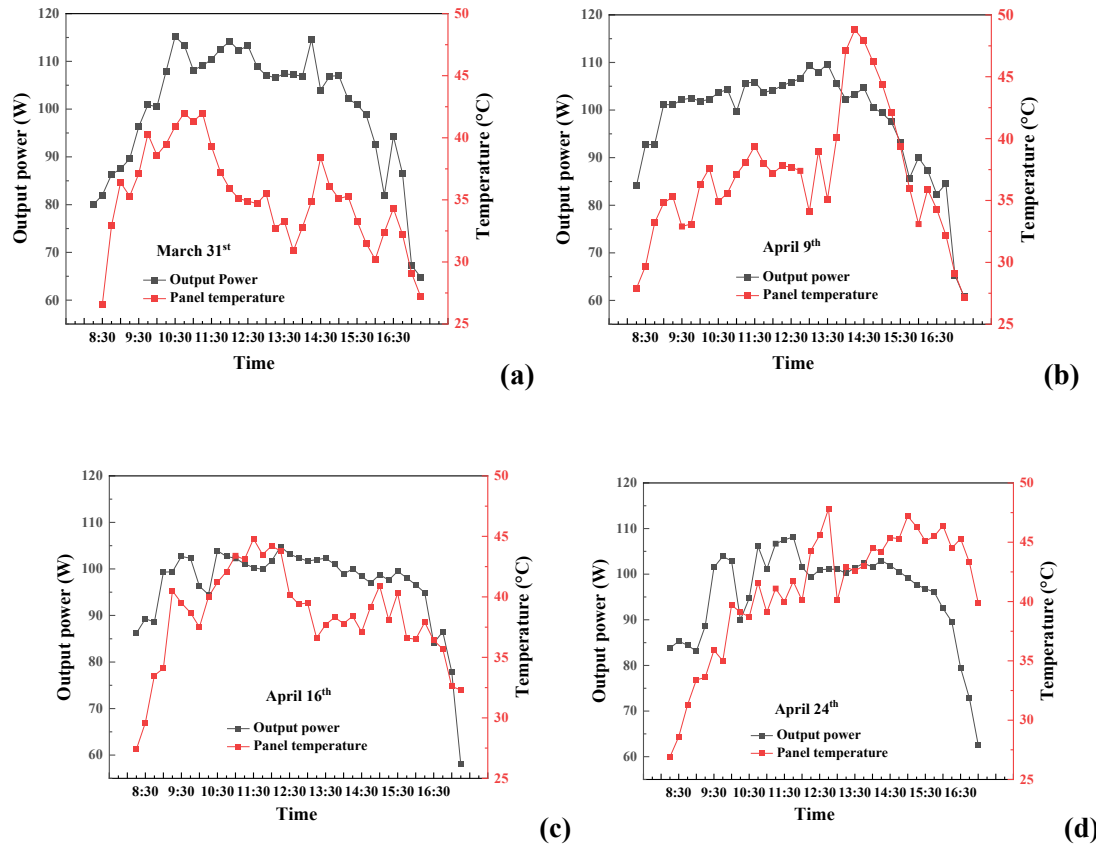


**Figure 8.** The relationship between solar cell output power and panel temperature in (a) March 31, (b) April 9, (c) April 16, and (d) April 24.

Figure 8 shows a general trend in which the power output of the solar panel gradually increases in the morning to reach the maximum value at noon; this is maintained for a period of time and then decreases gradually in the afternoon. Solar irradiation intensity definitely contributes to this trend; however, it is not the sole factor determining power output. For instance, as shown in Figure 8(b), a clear increase in panel temperature between 13:30 and 14:00 indicates an intensified solar irradiation, while the power output profile decreases. It is deduced, therefore, that the solar panel temperature plays an important role in PV power generation performance as well.

Based on the results shown in Figure 8(a)–(d), a clear negative relationship between the panel temperature and the solar panel power output can be observed. As shown in Figure 8(a),(c), although the panel temperature decreases in the noon period (13:00–15:00) due to cloudy weather, power output is maintained at a high level. On the contrary, as seen in Figure 8(b),(d), corresponding to April 9 and April 24, the elevated panel temperature during the period of 13:30–15:30 corresponds to a decreased electricity output performance. In addition, as shown in Figure 7, the largest daily power generation occurred on March 31, which had the lowest average ambient temperature of 11 °C and the consequent lowest panel temperature of 34.7 °C among the four study days. In the other three days, the lower panel temperature also corresponded to higher daily power output. For instance, the increasing daily-averaged solar panel temperatures from 36.9 °C on April 9 and 38.3 °C on April 16 to 40.9 °C on April 24 correspond precisely to the descending daily power output in these days. It is roughly estimated that

within the range of 34.7–40.9 °C, every 1 °C increase in panel temperature would lead to a 1% decrease in the daily power generation amount.

### 3.3.2. PV conversion efficiency

To quantify the negative correlation between solar panel temperature and solar cell power output, the dependence of the PV conversion efficiency, which is defined as the ratio of generated power over the total received sun irradiation, on the panel temperature, was investigated. The measurements were performed in three consecutive days from May 1 to May 3, and the results are displayed in Figure 9(a)–(c).

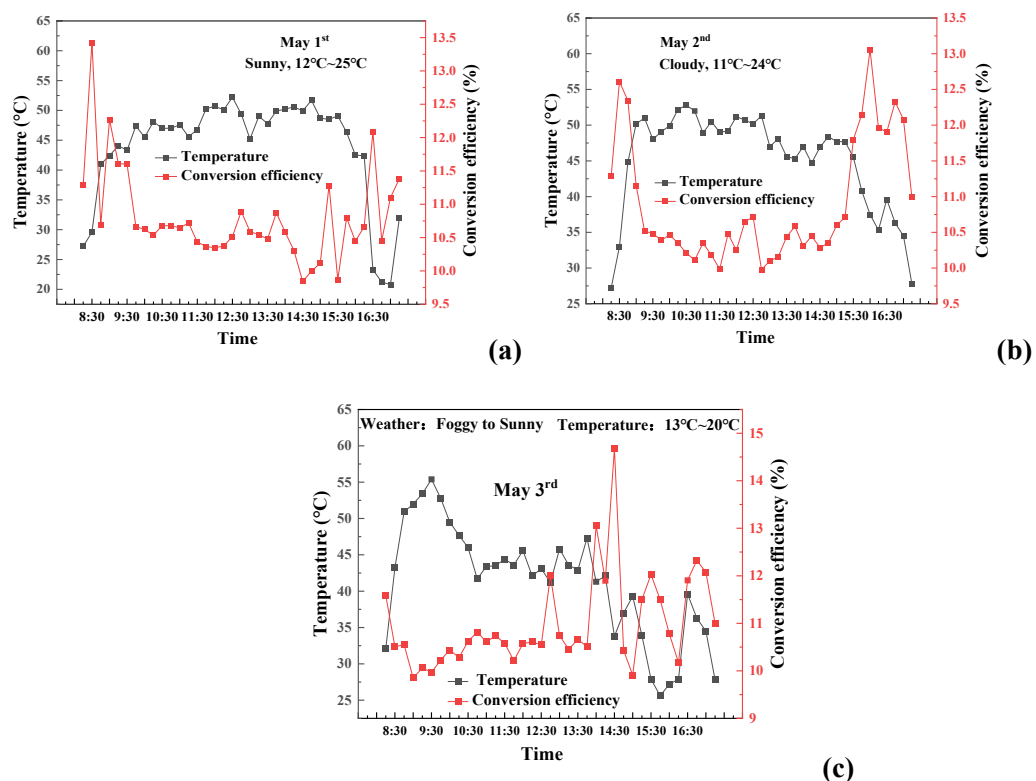


**Figure 9.** Relationship between solar cell PV conversion efficiency and panel temperature on (a) May 1, (b) May 2, and (c) May 3 of 2024.

Figure 9 shows that, in response to the gradually increasing solar irradiation in the morning and the gradually decreasing solar irradiation in the afternoon, the solar panel temperature varied accordingly in the range of 20–50 °C, 25–53 °C, and 25–55 °C for each of the three days. In the same figure, the negative relationship between panel temperature and PV conversion efficiency can be clearly observed. In Figure 9(a), the results on May 1 show that the energy conversion efficiency drops from the maximum of 13.4% to 10.5% along with an increasing panel temperature from 29 to 52 °C. Figure 9(b),(c) shows that, for the other two days, the same tendency occurs between panel temperature and PV conversion efficiency. In summary, the solar panel temperature elevation within the range of 20–55 °C obviously suppressed the PV conversion efficiency within the range of 9.8%–14.7%.

### 3.4. Discussion

An in-depth analysis of the factors that influence solar cell electricity power output is an important basis for a more efficient development of the solar energy field.

Solar light intensity definitely plays an important role in solar panel power output; the greater the amount of sunlight received by the panel, the more electricity the solar panel produces. The intensity of sunshine at the noon period surpassed 1000 watts per square meter, obviously higher than in the morning and afternoon periods. This resulted in time-dependent power output profiles, as shown in Figure 4(a)–(b), Figure 6(a)–(d), and Figure 9(a)–(c). The higher sun irradiation amount also led to a higher daily power output in the spring than in the winter, as revealed in Figures 5 and 7.

Additionally, based on the results reported in Section 3.3, the panel temperature is another key factor for solar cell PV conversion efficiency. More specifically, in the studied temperature range of 20–55 °C, increasing panel temperature resulted in an obvious decrease in solar cell PV conversion efficiency from ~15% to ~10%. This experimental observation is consistent with Cuce [40], who reported that a dramatic open circuit and maximum voltage decrease with increasing cell temperature. The physical mechanisms behind such negative correlation between cell temperature and power output capacity can be attributed to the following three aspects: 1) the bandgap width of silicon decreases accordingly with the increasing panel temperature, which results in a decrease in photo-generated carrier energy and thus a decrease in the output voltage; 2) the higher temperature enhances the activity of defect states and consequently excites the non-radiative recombination process of the non-equilibrium carrier, which releases the energy mainly in the form of heat and therefore results in decreased electricity power output; and 3) the energy dissipated in the form of heat inside the solar panel increases at higher temperature conditions, which leads to decreased energy to be converted into electricity [41–45].

Panel temperature control studies have become an interesting research topic in recent years. Ahmad et al. [46] designed a water-cooling PV system and reported a 10.35% increase in cell efficiency in comparison to the non-cooled panel. Rubaiee and Fazal [47] reported that the phase-change material (PCM) cooling system-integrated PV solar module could generate higher electricity. Basem [48] comprehensively analyzed four panel cooling methods and reported the most effective approach between water spray over the air, water, and nano-fluid cooling methods. Hamed et al. [49] introduced a new adsorption/desorption and heat sink method to cool the solar panel and obtained an enhanced power generation capacity of 29.8%. Ahmed et al. [50] overviewed popular solar cell cooling technologies, including passive cooling, active cooling, PCM cooling, and surface water spray cooling, among others, and pointed out that future research should focus on hybrid cooling approaches and explore new PCM materials.

Therefore, it is concluded that when considering the positive effects of light on power, the negative effects of the panel temperature cannot be ignored. In other words, an increase in panel temperature in combination with high light intensity may partially offset the power generation capacity. It is expected that future PV power generation systems may consider some panel temperature management parts to achieve maximum solar power harvest efficiency.

#### 4. Conclusions

In this paper, the solar panel power generation enhancement performance of an LDR-based DASTS was experimentally investigated. Special attention was placed on its performance in different seasons. The panel temperature effect on the PV power output was quantified as well. The following conclusions were drawn:

- (1) The DASTS clearly enhanced power output, especially in the morning and afternoon periods, regardless of season. In the winter, the daily power output from the DASTS was 9.9%–12.1% higher than that of the fixed panel system. In the spring, the power generation enhancement ratio of the DASTS was 30.6%–31.8% higher than that of the fixed panel system.
- (2) The panel temperature had a clear negative impact on PV conversion efficiency and power output of the solar cell panel. In the spring, PV conversion efficiency dropped from the maximum value of 14.7% to 9.8% along with an increasing panel temperature in the range of 20 to 55 °C.

It was demonstrated that the DASTS is technically feasible to improve the power generation efficiency of solar panels. In addition, it is advised that a panel temperature management system is applied in the future to achieve maximal solar power harvesting efficiency.

#### Use of AI tools declaration

The authors declare they have not used Artificial Intelligence (AI) tools in the creation of this article.

#### Acknowledgments

The paper is finished under the Graduate Tutor Foundation of Qingdao University of Science and Technology (120202190414).

#### Conflict of interest

The authors declare that there are no conflicts of interest regarding the publication of this article.

#### Reference

1. Cao J, Zhang J, Chen Y, et al. (2023) Current status, future prediction and offset potential of fossil fuel CO<sub>2</sub> emissions in China. *J Cleaner Prod* 426: 139207. <https://doi.org/10.1016/j.jclepro.2023.139207>
2. Liu J, Ma X, Zhao B, et al. (2024) Steering toward sustainability: Can dual circulation development mitigate CO<sub>2</sub> emissions?—Evidence from China. *J Cleaner Prod* 474: 143548. <https://doi.org/10.1016/j.jclepro.2024.143548>
3. Du D, Zhao D, Li Y, et al. (2021) Parameter calibration of the stochastic bubble population balance model for predicting NP-stabilized foam flow characteristics in porous media. *Colloids Surf. A* 614: 126180. <https://doi.org/10.1016/j.colsurfa.2021.126180>

4. Li Y, Zhao D, Du D (2022) Computational study on the three phase displacement characteristics of foam fluids in porous media. *J Pet Sci Eng* 215: 110732. <https://doi.org/10.1016/j.petrol.2022.110732>
5. Song X, Cui X, Jiang L, et al. (2022) Multi-parameter screening study on the static properties of nanoparticle-stabilized CO<sub>2</sub> foam near the CO<sub>2</sub> critical point. *Arabian J Chem* 15: 103676. <https://doi.org/10.1016/j.arabjc.2021.103676>
6. Wang D, Yang M, Su X, et al. (2025) A mechanistic investigation on NP-stabilized foam three phase displacement characteristics in low permeable porous media. *Geoenergy Sci Eng* 245: 213526. <https://doi.org/10.1016/j.geoen.2024.213526>
7. Zang H, Yan S, Liu Z, et al. (2025) Determination of the minimum miscibility pressures of CO<sub>2</sub> and multicomponent oil system with a novel diffusion coefficient fit line intersection methodology. *Fuel* 385: 134106. <https://doi.org/10.1016/j.fuel.2024.134106>
8. Haugen M, Blaisdell-Pijuan PL, Botterud A, et al. (2024) Power market models for the clean energy transition: State of the art and future research needs. *Appl Energy* 357: 122495. <https://doi.org/10.1016/j.apenergy.2023.122495>
9. Lane K, Daouda M, Yuan A, et al. (2024) Readiness for a clean energy future: Prevalence, perceptions, and barriers to adoption of electric stoves and solar panels in New York city. *Energy Policy* 194: 114301. <https://doi.org/10.1016/j.enpol.2024.114301>
10. Pourasl HH, Barenji RV, Khojastehnezhad VM (2023) Solar energy status in the world: A comprehensive review. *Energy Rep* 10: 3474–3493. <https://doi.org/10.1016/j.egyr.2023.10.022>
11. AL-Rousan N, Isa NAM, Desa MK M (2018) Advances in solar photovoltaic tracking systems: A review. *Renewable Sustainable Energy Rev* 82: 2548–2569. <https://doi.org/10.1016/j.rser.2017.09.077>
12. Bahrami A, Okoye C, Pourasl HH, et al. (2022) Techno-economic comparison of fixed and tracking flat plate solar collectors in the northern hemisphere. *J Cleaner Prod* 378: 134523. <https://doi.org/10.1016/j.jclepro.2022.134523>
13. Hafez AZ, Yousef AM, Harag NM (2018) Solar tracking systems: Technologies and trackers drive types—A review. *Renewable Sustainable Energy Rev* 91: 754–782. <https://doi.org/10.1016/j.rser.2018.03.094>
14. Kumba K, Upender P, Buduma P, et al. (2024) Solar tracking systems: Advancements, challenges, and future directions: A review. *Energy Rep* 12: 3566–3583. <https://doi.org/10.1016/j.egyr.2024.09.038>
15. Paliyal PS, Mondal S, Layek S, et al. (2024) Automatic solar tracking system: A review pertaining to advancements and challenges in the current scenario. *Clean Energy* 8: 237–262. <https://doi.org/10.1093/ce/zkae085>
16. Wang S, Shen Y, Zhou J, et al. (2022) Efficiency enhancement of tilted bifacial photovoltaic modules with horizontal single-axis tracker—The bifacial companion method. *Energies* 15. <https://doi.org/10.3390/en15041262>
17. Khandekar M, Muthyalu S, Agashe S, et al. (2023) Development of an intelligent sun tracking system for solar pv panel. In: *2023 IEEE IAS Global Conference on Emerging Technologies*. <https://doi.org/10.1109/GlobConET56651.2023.10149926>
18. Abdul-Ghafoor QJ, Abed SH, Kadhim SA, et al. (2024) Experimental and numerical study of a linear Fresnel solar collector attached with dual axis tracking system. *Results Eng* 23: 102543. <https://doi.org/10.1016/j.rineng.2024.102543>

19. Al-Amayreh MI, Alahmer A (2022) On improving the efficiency of hybrid solar lighting and thermal system using dual-axis solar tracking system. *Energy Rep* 8: 841–847. <https://doi.org/10.1016/j.egyr.2021.11.080>
20. Kumar S, Thakur R, Lee D, et al. (2024) Impact of liquid spectrum filter and solar tracker on the overall effectiveness of a photovoltaic thermal system: An experimental investigation. *Renewable Energy* 226: 120390. <https://doi.org/10.1016/j.renene.2024.120390>
21. Maliani O, Bekkaoui A, Baali E, et al. (2020) Investigation on novel design of solar still coupled with two axis solar tracking system. *Appl Therm Eng* 172: 115144. <https://doi.org/10.1016/j.aplthermaleng.2020.115144>
22. Mamodiya U, Tiwari N (2023) Dual-axis solar tracking system with different control strategies for improved energy efficiency. *Comput Electr Eng* 111: 108920. <https://doi.org/10.1016/j.compeleceng.2023.108920>
23. Fathabadi H (2016) Novel high efficient offline sensorless dual-axis solar tracker for using in photovoltaic systems and solar concentrators. *Renewable Energy* 95: 485–494. <https://doi.org/10.1016/j.renene.2016.04.063>
24. Sidek M, Azis N, Hasan W, et al. (2017) Automated positioning dual-axis solar tracking system with precision elevation and azimuth angle control. *Energy* 124: 160–170. <https://doi.org/10.1016/j.energy.2017.02.001>
25. Jamroen C, Fongkerd C, Krongpha W, et al. (2021) A novel UV sensor-based dual-axis solar tracking system: Implementation and performance analysis. *Appl Energy* 299: 117295. <https://doi.org/10.1016/j.apenergy.2021.117295>
26. Ponce-Jara MA, Velásquez-Figureueroa C, Reyes-Mero M, et al. (2022) Performance comparison between fixed and dual-axis sun-tracking photovoltaic panels with an IoT monitoring system in the coastal region of ecuador. *Sustainability* 14: 1696. <https://doi.org/10.3390/su14031696>
27. Andriamahefa MH, Bourdin V, Mininger X, et al. (2023) Control strategy for a dual-axis sun tracker based on a radiometric cube to maximize the power output of the PV system. *EPJ Photovoltaics* 14: 35. <https://doi.org/10.1051/epjpv/2023022>
28. Jaafar SS, Maarof HA, Hamasalh HB, et al. (2024) Comparative performance evaluation of dual-axis solar trackers: Enhancing solar harvesting efficiency. *J Mechatron Electr Power Veh Technol* 15: 23–31. <https://doi.org/10.55981/j.mev.2024.808>
29. Nguyen B, Ho H (2020) Design, implementation and performance analysis of a dual axis solar tracking system. *Adv Sci Technol Eng Systs* 5: 41–45. <https://doi.org/10.25046/aj050306>
30. Zhu Y, Liu J, Yang X (2020) Design and performance analysis of a solar tracking system with a novel single-axis tracking structure to maximize energy collection. *Appl Energy* 264: 114647. <https://doi.org/10.1016/j.apenergy.2020.114647>
31. Riyadi T, Effendy M, Utomo B, et al. (2023) Performance of a photovoltaic-thermoelectric generator panel in combination with various solar tracking systems. *Appl Therm Eng* 235: 121336. <https://doi.org/10.1016/j.aplthermaleng.2023.121336>
32. Fuentes-Morales RF, Diaz-Ponce A, Peña-Cruz MI, et al. (2020) Control algorithms applied to active solar tracking systems: A review. *Solar Energy* 212: 203–219. <https://doi.org/10.1016/j.solener.2020.10.071>
33. Anshory I, Jamaaluddin J, Fahruddin A, et al. (2024) Monitoring solar heat intensity of dual axis solar tracker control system: New approach. *Case Stud Therm Eng* 53: 103791. <https://doi.org/10.1016/j.csite.2023.103791>

34. Kuttybay N, Mekhilef S, Koshkarbay N, et al. (2024) Assessment of solar tracking systems: A comprehensive review. *Sustainable Energy Technol Assess* 68: 103879. <https://doi.org/10.1016/j.seta.2024.103879>

35. Lu W, Ajay P (2024) Solar PV tracking system using arithmetic optimization with dual axis and sensor. *Meas Sens* 33: 101089. <https://doi.org/10.1016/j.measen.2024.101089>

36. Vaziri Rad MA, Toopshekan A, Rahdan P, et al. (2020) A comprehensive study of techno-economic and environmental features of different solar tracking systems for residential photovoltaic installations. *Renewable Sustainable Energy Rev* 129: 109923. <https://doi.org/10.1016/j.rser.2020.109923>

37. Jamroen C, Komkum P, Kohsri S, et al. (2020) A low-cost dual-axis solar tracking system based on digital logic design: Design and implementation. *Sustainable Energy Technol Assess* 37: 100618. <https://doi.org/10.1016/j.seta.2019.100618>

38. Karabiber A, Guñes Y (2023) Single-motor and dual-axis solar tracking system for micro photovoltaic power plants. *J Solar Energy Eng Trans ASME* 145: 051004. <https://doi.org/10.1115/1.4056739>

39. Song G, Han D, Li Y, et al. (2024) Enhancement of solar panel power generation performance with a passive sun tracking system. *Therm Sci Eng* 7: 7906. <https://doi.org/10.24294/tse.v7i1.7906>

40. Cuce E, Cuce PM, Bali T (2013) An experimental analysis of illumination intensity and temperature dependency of photovoltaic cell parameters. *Appl Energy* 111: 374–382. <https://doi.org/10.1016/j.apenergy.2013.05.025>

41. Gindi O, Fradkin Z, Itzhak A, et al. (2023) Lowering the temperature and increasing the fill factor of silicon solar cells by filtering of sub-bandgap wavelengths. *Energies* 16. <https://doi.org/10.3390/en16155631>

42. Hassan S, Omer M, Mofdal M (2025) Determining the Efficiency of Solar Cells at Different Temperatures. *J Power Energy Eng* 13: 23–32. <https://doi.org/10.4236/jpee.2025.134003>

43. Karmani Y, Bilal M, Salman M, et al. (2025) Correlation between trap-assisted non-radiative recombination losses and thermal agitation in SnS-based solar cell: A state-of-the-art computational analysis. *Mater Sci Eng B* 321: 118484. <https://doi.org/10.1016/j.mseb.2025.118484>

44. Shaker L, Al-Amiry A, Hanoon M, et al. (2024) Examining the influence of thermal effects on solar cells: A comprehensive review. *Sustainable Energy Res* 11: 6. <https://doi.org/10.1186/s40807-024-00100-8>

45. Si X, Shi W, Wang R, et al. (2024) Suppressing non-radiative recombination and tuning morphology via central core asymmetric substitution for efficient organic solar cells. *Nano Energy* 131: 1–8. <https://doi.org/10.1016/j.nanoen.2024.110204>

46. Ahmad N, Khandakar A, El-Tayeb A, et al. (2018) Novel design for thermal management of PV cells in harsh environmental conditions. *Energies* 11: 3231. <https://doi.org/10.3390/en11113231>

47. Rubaiee S, Fazal MA (2022) The influence of various solar radiations on the efficiency of a photovoltaic solar module integrated with a passive cooling system. *Energies* 15: 9584. <https://doi.org/10.3390/en15249584>

48. Basem A, Mukhtar A, Elbarbary ZMS, et al. (2024) Experimental study on the various varieties of photovoltaic panels (PVs) cooling systems to increase their electrical efficiency. *PLoS One* 19: e0307616. <https://doi.org/10.1371/journal.pone.0307616>

49. Hamed MH, Hassan H, Ookawara S, et al. (2024) Performance comparative study on passively cooled concentrated photovoltaic (PV) using adsorption/desorption and heat sink cooling methods: Experimental investigations. *Energy* 307: 132700. <https://doi.org/10.1016/j.energy.2024.132700>
50. Ahmed YE, Maghami MR, Pasupuleti J, et al. (2024) Overview of recent solar photovoltaic cooling system approach. *Technologies* 12: 171. <https://doi.org/10.3390/technologies12090171>



AIMS Press

© 2025 the Author(s), licensee AIMS Press. This is an open access article distributed under the terms of the Creative Commons Attribution License (<https://creativecommons.org/licenses/by/4.0>)